ELSEVIER

Contents lists available at ScienceDirect

Soil Biology and Biochemistry

journal homepage: www.elsevier.com/locate/soilbio



Research Paper

Modelling mycelial responses to nitrogen limitation during litter decomposition

Samia Ghersheen a,*, Stefano Manzoni b, Marie Spohn a, Björn D. Lindahl a

- ^a Swedish University of Agricultural Sciences, Department of Soil and Environment, PO Box 7014, SE-750 07, Uppsala, Sweden
- b Stockholm University, Department of Physical Geography and Bolin Centre for Climate Research, Stockholm, SE-106 91, Sweden

ARTICLE INFO

Dataset link: https://doi.org/10.5281/zenodo.1

Keywords:
Litter decomposition
N limitation
Mathematical modelling
Mycelial dynamics
Decomposer fungi
Fungal necromass

ABSTRACT

Most soil organic matter models focus on carbon (C) dynamics rather than on element interactions. However, in many regions of the world, particularly at high latitudes, soil organic matter decomposition is constrained by low nitrogen (N) availability. This phenomenon is not well understood and usually not mechanistically represented in decomposition models. Here we formulated a process-based model of litter decomposition to investigate N limitation effects on fungus-driven decomposition. Unlike most other decomposition models, our model describes fungal mycelial dynamics explicitly. Fungal biomass is divided into three fractions: (1) cytoplasmic cells active in decomposition, (2) vacuolised cells with a lower N content and without decomposition capacity, and (3) dead cells (necromass). The model can predict mass loss trajectories of litter types with different N content based on site-specific parameters. The fungal mycelium responds to N limitation by increasing the proportion of vacuolised, inactive cells with a low N content, reducing decomposition rates. As a consequence of increased cell inactivation under N limitation, N accumulates in the necromass pool. To predict observed patterns of N immobilisation and release, the rate of fungal necromass decomposition has to be slow and close to that of lignin. Moreover, we found that slow mycelial growth facilitates exploitation of low N resources, whereas fast growth intensifies N-limitation. Our model disentangles the interplay between N availability, mycelial dynamics, and decomposition, pointing towards the potentials of more explicit incorporation of fungal traits in models of N limited ecosystems.

1. Introduction

Variation in nitrogen (N) availability plays a central role in regulation of litter decomposition. Decomposer growth and activity are often constrained by low N availability during early stages of decomposition (Berg and McClaugherty, 2008; Melillo et al., 1982). Slow decomposition, in turn, impedes N mineralisation and leads to N retention in organic matter pools with a potential for amplifying feedbacks — as more N and carbon (C) accumulate in organic matter, even less N becomes available for plants and decomposers. When these feedbacks occur, ecosystems can enter a retrogressive phase, with gradually declining productivity until a disturbance breaks the cycle (Clemmensen et al., 2013; Kyaschenko et al., 2019; Wardle et al., 2003). However, given the limited number of large scale and long term experiments or monitoring sites, the potential for below-ground C storage in N limited ecosystems, as a climate mitigation strategy, remains challenging to predict. Ecosystem dynamics in such conditions can be examined with coupled C-N cycling models, but to capture N limitation feedbacks, such models need to explicitly represent decomposers and their responses to N availability.

Litter decomposition is influenced by combined effects of substrate composition and the associated microbial responses. Microorganisms are affected by stoichiometric imbalances that may result from shortage of N rich compounds, and their responses to this imbalance mediates the interplay between C and N during decomposition (Mooshammer et al., 2014). Therefore, to account for the influence of N availability on decomposition in ecosystem models, decomposer response traits have to be explicitly represented (Bradford et al., 2017). Microbial communities may deal with the challenge of stoichiometric imbalances by different strategies, such as: (1) adjustment of biomass composition to their resource (within physiological boundaries) (Camenzind et al., 2021), (2) selective resource use by altered production of different extracellular enzymes (Mooshammer et al., 2014; Moorhead et al., 2013), (3) regulation of C vs. N losses; e.g., through respiration (flexible carbon use efficiency, CUE, defined as the ratio between growth and C uptake) and N mineralisation (Manzoni et al., 2017; Mooshammer et al., 2014),

E-mail address: samia.ghersheen@slu.se (S. Ghersheen).

^{*} Corresponding author.

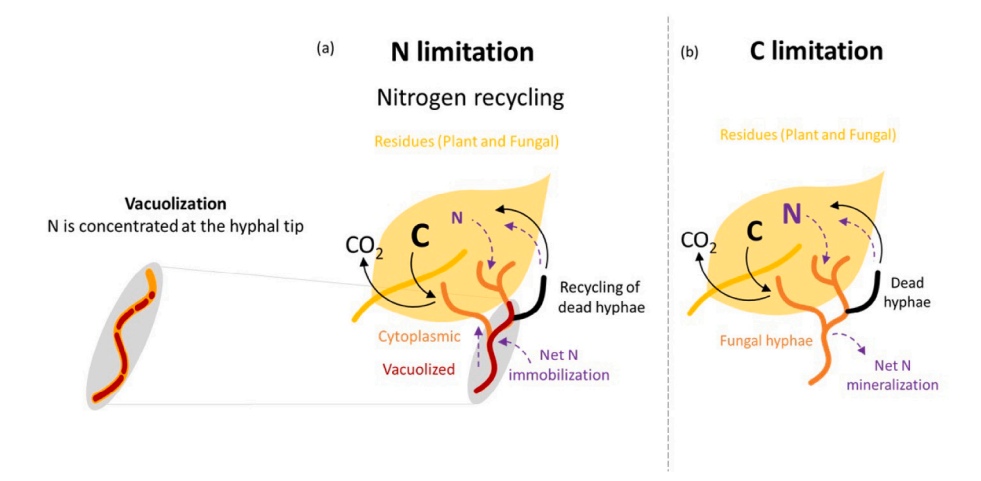


Fig. 1. When N limited, fungi use the mechanisms of vacuolisation (which is linked to N reallocation to growing hyphal tips), N recycling from dead hyphae and N uptake from the environment (if available) to acquire additional N for growth (a), whereas under C-limitation, excess N is released (b).

(4) retention of N at senescence under N limitation (Camenzind et al., 2023), or (5) import of N into N-poor litter during early stages of decomposition (Spohn and Berg, 2023).

Decomposition models dealing with stoichiometric imbalances commonly feature one or more of these adaptive strategies to investigate the effect of nutrient limitation (Fatichi et al., 2019; Manzoni et al., 2017; Mooshammer et al., 2014; Parton et al., 1993; Sistla et al., 2014b). In an attempt to compare the above mentioned microbial response strategies to handle N limitation, Manzoni et al. (2021) implemented them in a common model platform. However, all model variants provided equally good fit to litter decomposition data, regardless of the implemented microbial response, and much ambiguity remains about the mechanisms at play.

Decomposition of litter and particulate organic matter is dominated by fungi, which are also particularly prominent in ecosystems characterised by strong N limitation (Baldrian, 2017). Fungal biomass dynamics and the ability to redistribute resources in mycelial networks accentuate their significance in linking the terrestrial C and N cycles (Boberg et al., 2014; Guhr et al., 2015; Spohn and Berg, 2023). While models of fungal growth behaviour are rare, there are some good examples (Boswell et al., 2002; Falconer et al., 2005, 2007), which include e.g growth, branching and anastomosis as well as mechanisms of hyphal resource translocation. These models focus on the development of mycelial morphology without including any feedback on decomposition. In contrast to models of fungal morphology, decomposition models rarely feature explicit feedbacks via decomposers traits. For example, in the model of Manzoni et al. (2021), mycelial N content reflected the N content of utilised resources but without any direct consequences for decomposition. Here we merge both approaches by linking fungal morphological features that allow coping with N limitation to decomposition.

Fungi can adapt to N shortage in many different ways (Boberg et al., 2014; Lindahl et al., 2002; Veses et al., 2008). In contrast to other microorganisms, they are usually multicellular and have a well developed capacity to redistribute resources in their mycelium, from sites of abundance (sources) to sites of scarcity (sinks), thereby optimising their overall performance (Boberg et al., 2014; Boddy, 1999; Fricker et al., 2017; Lindahl and Olsson, 2004). The fungal cytoplasm is relatively rich in N, but as hyphal cells age, they may gradually be filled with large vacuoles with a more dilute N content. The purpose of these vacuoles is to maintain cell turgor and viability with a minimal expenditure of resources. Replacement of cytoplasm with vacuoles results in cells with a lower N content, and displacement of cytoplasm towards the N-rich growing hyphal tips (Fig. 1) is a way to maintain growth in the face of nutrient shortage (Veses et al., 2008).

The different N content of cytoplasmic vs. vacuolised cells allows some plasticity in the total fungal biomass C:N ratio, despite individual cell types being homeostatic. There is indeed evidence of some increase in microbial C:N in response to N limitation (Camenzind et al., 2021; Manzoni et al., 2010; Högberg et al., 2021), especially when fungi grow on particulate organic matter (Tipping et al., 2016) and litter (Berg and McClaugherty, 2008). Fungi may also recycle resources and minimise accumulation of N in senescent mycelium by controlling their own cell mortality, allowing older hyphae or entire sections of their mycelium to die, while reallocating resources to mycelium in new and attractive resources (Dowson et al., 1989; Fricker et al., 2017).

The efficient reallocation of N from senescing mycelium to growing hyphal tips was illustrated by autoradiographic imaging of radiolabelled amino acids (Tlalka et al., 2008); as a mycelial front advanced across the substrate, few labelled nutrient-rich amino acids were left behind, as nutrients were continuously redistributed to the mycelial front. Such dynamic nutrient reallocation has to depend on highly efficient mechanisms that shift cytoplasm towards the hyphal tips (i.e. vacuolisation), recycle resources from senescing cells, and decompose and recycle cell walls of dead mycelium (Fig. 1a).

In this contribution, we develop a process-based model of litter or particulate organic matter decomposition that incorporates adaptive fungal mycelial dynamics. The model is used to examine if such dynamics can capture the negative effect of N limitation on C losses during early stages of decomposition. We focus on these mycelial processes instead of regulation of C metabolism, such as a decrease in CUE in response to N limitation. Lowering of CUE due to overflow metabolism (Manzoni et al., 2017; Schimel and Weintraub, 2003) is a wasteful strategy and less likely to provide an evolutionary advantage compared to plastic N retention. Selective production of N liberating enzymes relative to C targeting enzymes may seem more likely, but fungal hyphae in litter have to decompose structural carbohydrates to proliferate in the substrate, even when C is abundant in excess of demand. Previous studies that explored how soil microorganisms cope with an unfavourable stoichiometry of their substrate pointed out that recycling of nutrients might play a major role for microbial growth under low nutrient availability (Manzoni et al., 2021; Spohn and Widdig, 2017). Here we explore these ideas further in a model that describe internal transfer of N and C between different pools of fungal mycelium. We assume that N limitation does not manifest as lower CUE or selective mobilisation of N from decomposing litter, but that N limitation induces alteration of the mycelium into a non active (vacuolised) state with lower N content. Moreover, N can only be immobilised in living microbial biomass, but long term N retention depends on the decomposition rate of microbial necromass (Baldrian

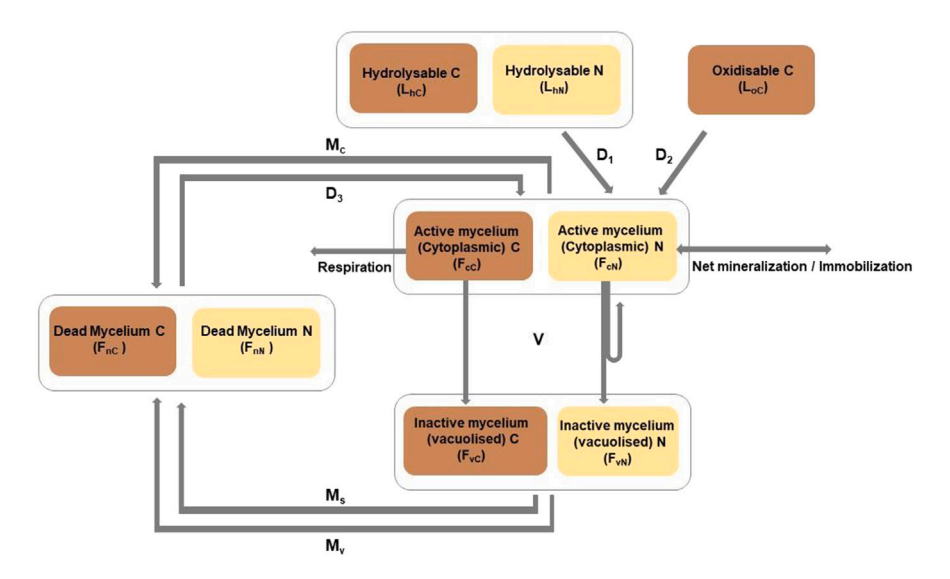


Fig. 2. Schematic of flows of carbon (C) and nitrogen (N) between different pools, each decomposing at different rates D_i , i = 1, 2, 3. The fungal biomass F_{cC} and F_{cN} represent represent C and N amounts in cytoplasmic cells with high decomposer activity; Foc. and Fon. represent C and N amounts in vacuolized cells with a lower N content and no decomposer activity; F_{nC} and F_{nN} represent C and N amounts in dead fungal cells. Vacuolisation of fungal mycelium (V) implies retention of nitrogen in cytoplasmic mycelium, since the vacuolised mycelium has a lower N content.

et al., 2013; Fernandez and Kennedy, 2018). Therefore, necromass is considered as a separate pool in the model, allowing us to investigate how modulation of necromass decomposition impacts N dynamics.

We hypothesise that explicit representation of hyphal vacuolisation, adaptive N content of different cell types (allowing plastic C:N at the whole mycelium scale), and increased mortality of senescent tissues enables prediction of decomposition patterns of litters with contrasting N content with a single parameter set (at a given site) and without the need to vary CUE or allow for selective acquisition of C or N. Fungal necromass often contains melanin or may be complexed with tannins (Adamczyk et al., 2019), retarding its decomposition (Baskaran et al., 2019). Thus, we also hypothesised that necromass decomposition is slow with rates more similar to those of lignin than to those of the more easily decomposable cellulose or proteins.

2. Methods

We begin by outlining the model structure including key assumptions, model schematic, parameters and C, N flow rates in Section 2.1 Model structure and assumptions. Following this, the Section 2.2 Model analysis details the fungal dynamics in response to C and N limitation. Finally, we describe model parametrisation based on data from two common garden litter bag decomposition experiments (Berg and McClaugherty, 1989; Osono and Takeda, 2004), using the generalised likelihood uncertainty estimation (GLUE) method (Section 2.3 Model parametrisation and goodness of fit). A detailed description of model variables, fluxes, and parameters, is given in Table 1, Table 2, and Table

2.1. Model structure and assumptions

Our model is grounded on two key assumptions: instead of using flexible CUE and/or selective resource acquisition via variable enzyme production, we assume that CUE and relative decomposition of C and N are fixed. Rather, our model focuses on mycelial dynamics and N transfer within the mycelium, which are assumed to be the main avenue of fungal response to N limitation. Plant litter tissues are divided into two pools of different quality (Fig. 2): a hydrolysable pool (fast decomposing litter components such as cellulose and proteins, L_h), and an oxidisable pool (recalcitrant litter compounds that cannot be hydrolysed, such as lignin, L_o). The hydrolysable pool contains both C and

N (L_{hC}, L_{hN}) , whereas the oxidisable pool contains only carbon L_{oC} . Fungal mycelial dynamics is incorporated by considering three different fractions of fungal mycelium (Fig. 2): active, vacuolised, and dead, describing the different states of fungal cells: N-rich cytoplasmic cells that can decompose organic substrates (active cells, F_c), vacuolised cells with a lower N content and without decomposer activity (inactive cells, F_n), and dead cells (necromass subjected to decomposition, F_n). The dead organic matter pools (hydrolysable and oxidisable plant litter as well as fungal necromass) are decomposed with the specific rates D_i (i = 1, 2, 3) and contribute to the production of fungal biomass after respiratory losses according to CUE. In case of C limitation, excess N is released by mineralisation. When organic N is not sufficient to fulfil fungal requirements, N can also be imported from the environment. If N import is not enough, N limitation ensues, and a fraction of the fungal biomass is vacuolised with the rate V, creating an inactive biomass pool with lower N content. Both cytoplasmic and vacuolised mycelial fractions are subject to mortality in proportion to standing biomass, M_i (i = c, v), but mortality of vacuolised mycelium can be increased by senescence (M_s) . Dead mycelium does not return to a common litter pool but forms a distinct necromass pool. The decomposition dynamics is then defined by the following system of differential equations, each representing the mass balance for C or N in one of the model compartments.

$$\frac{dL_{hC}}{dt} = -D_1,\tag{1}$$

$$\frac{dt}{dL_{hN}} = -D_1 \frac{L_{hN}}{L_{hC}},\tag{2}$$

$$\frac{dL_{oC}}{dt} = -D_2,\tag{3}$$

$$\frac{aF_{cC}}{dt} = \epsilon(D_1 + D_2 + D_3) - V - M_c,\tag{4}$$

$$\frac{dL_{oC}}{dt} = -D_2,$$

$$\frac{dF_{cC}}{dt} = \epsilon(D_1 + D_2 + D_3) - V - M_c,$$

$$\frac{dF_{cN}}{dt} = D_1 \frac{L_{hN}}{L_{hC}} + D_3 \frac{F_{nN}}{F_{nC}} - V \rho_2 - M_c \rho_1 - \phi,$$
(5)

$$\frac{dP_{vC}}{dt} = V - M_v - M_s,\tag{6}$$

$$\frac{dI_{vN}}{dt} = (V - M_v - M_s)\rho_2,\tag{7}$$

$$\frac{dF_{nC}}{dt} = M_c + M_v + M_s - D_3,\tag{8}$$

$$\frac{dF_{vC}}{dt} = V - M_v - M_s,$$
(6)
$$\frac{dF_{vN}}{dt} = (V - M_v - M_s)\rho_2,$$
(7)
$$\frac{dF_{nC}}{dt} = M_c + M_v + M_s - D_3,$$
(8)
$$\frac{dF_{nN}}{dt} = M_c \rho_1 + (M_v + M_s)\rho_2 - D_3 \frac{F_{nN}}{F_{nC}},$$
(9)

Table 1
State variables (mg).

Symbol	Description	
L_{hC}	Hybridisable litter C	
L_{hN}	Hydrolysible litter N	
L_{oC}	Oxidisable litter C	
F_{cC}	C amount of cytoplasmic mycelium	
F_{cN}	N amount of cytoplasmic mycelium	
$F_{\nu C}$	C amount of vacuolised mycelium	
F_{vN}	N amount of vacuolised mycelium	
F_{nC}	C amount in fungal necromass	
F_{nN}	N amount in fungal necromass	

where subscripts C and N denote carbon and nitrogen, D_i (i=1,2,3) represent decomposition rates of dead plant and fungal pools, M_j (j=c,v,s) represent mortality rates, V is the rate of conversion of mycelium from cytoplasmic to vacuolised, and ϕ is the net N mineralisation rate. To enable parametrisation using experimental litter bag data, the model does not feature external litter inputs, but represent the dynamics during decomposition of a single litter cohort (e.g. in a litter bag).

The decomposition rates (D_1, D_2, D_3) of plant (L_h, L_o) and fungal necromass (F_n) pools are defined by kinetics similar to the equilibrium chemistry approximation (Tang and Riley, 2013), in which decomposition rates saturate at high mycelial biomass,

$$D_{1} = D_{max_{1}} \frac{L_{hC}F_{cC}}{K(L_{hC} + L_{oC} + F_{nC}) + F_{cC} + F_{vC}}$$

$$D_{2} = D_{max_{2}} \frac{L_{oC}F_{cC}}{K(L_{hC} + L_{oC} + F_{nC}) + F_{cC} + F_{vC}}$$

$$D_{3} = D_{max_{3}} \frac{F_{nC}F_{cC}}{K(L_{hC} + L_{oC} + F_{nC}) + F_{cC} + F_{vC}}$$
(10)

Maximum rates of decomposition of plant litter (D_{max_1} , D_{max_2}) and fungal necromass (D_{max_3}) occur only when these dead pools are saturated by active mycelium. Thus, decomposition rates (D_1, D_2, D_3) depend only on cytoplasmic cells F_c , whereas vacuolised cells, F_v , do not take part in the decomposition process but compete for space in the decomposing substrate. Furthermore, N and C in the dead litter pools decompose at the same relative rate (i.e. there is no preferential decomposition of N under N limitation). Fungal growth depends on resources made available by decomposition subjected to respiratory losses defined through the fungal CUE, ϵ . Cytoplasmic mycelium (F_c) is converted to vacuolised mycelium (F_v) with the rate V according to first-order kinetics with respect to F_c and a rate parameter α_v (Section 2.2). We consider a mortality pathway where both cytoplasmic (F_c) and vacuolised (F_v) mycelium are subject to equal mortality proportional to standing biomass (M_c, M_v) regulated by a first-order rate constant α_m , whereas F_v is also subject to mortality (M_s) associated with mycelial senescence regulated by the first-order rate constant β . The N:C ratios of cytoplasmic mycelium $\rho_1 = \frac{F_{cN}}{F_{cC}}$, and vacuolised

mycelium $\rho_2 = \frac{F_{vN}}{F_{vC}}$ are fixed and $\rho_1 > \rho_2$, since cytoplasmic cells have has a higher N content than vacuolised cells; therefore, vacuolisation decreases hyphal N content (Veses et al., 2008). The N pool of cytoplasmic mycelium F_{cN} is determined by inputs from decomposition and losses through vacuolisation and mortality. N losses through vacuolisation decrease with declining N content of vacuolised mycelium ρ_2 . Furthermore, the N pool in cytoplasmic mycelium F_{cN} can increase by immobilisation of N from the environment (negative values of the net N mineralisation rate ϕ) whereas surplus N can be mineralised (positive ϕ ; Section 2.2). In essence, vacuolisation leads to internal reallocation of N to active mycelium F_c , and senescence mortality M_s increases turn-over of the vacuolised mycelium F_{ν} , leading to recycling of N through decomposition of necromass. Note that the N:C ratios of all pools are constant, except for fungal necromass (F_n) , for which the N:C ratio depends on the relative contribution of cytoplasmic mycelium (through proportional mortality) and vacuolised mycelium (through proportional and senescence mortality).

2.2. Modelling fungal responses to N and C limitation

The net N mineralisation rate ϕ and the parameter α_v are autonomous (state dependent) quantities that have to be defined. ϕ enables release of excess N when fungi acquire a surplus of N (i.e. under C limitation; Fig. 1b), while α_v enables retention of N in active mycelium through vacuolisation when fungi experience N deficiency (Fig. 1a). This mechanism is based on the assumption that N:C of the cytoplasmic mycelium (active cells) is time invariant, and is implemented using the following expression, which is derived from Eqs. (4) and (5) by imposing $\frac{dF_{cN}}{dt} = \rho_1 \frac{dF_{cC}}{dt}$,

$$\phi = V\left(\rho_1 - \rho_2\right) + D_1 \frac{L_{hN}}{L_{hC}} + D_3 \frac{F_{nN}}{F_{nC}} - \epsilon \rho_1 (D_1 + D_2 + D_3). \tag{11}$$
 The Eq. (11) implies that N mineralisation depends on rates of de-

The Eq. (11) implies that N mineralisation depends on rates of decomposition, but is also modulated by the availability of, and demand for, N. Under conditions of high N availability (i.e. C limitation), we assume that V = 0 by setting α_v to 0 in (11), because no hyphal vacuolisation is needed. Under these conditions, ϕ attains positive values, representing release of excess N to the environment (i.e. net N mineralisation).

When the amount of N acquired from the litter (at a rate $D_1 \frac{L_{hN}}{L_{hC}} + D_3 \frac{F_{nN}}{F_{nC}}$) and from external N sources (at a maximum rate $-\phi_{min}$) is too low to fulfil the requirements of fungal mycelium, N becomes limiting for fungal growth. To implement N-limitation, we set $\phi = \phi_{min}$ in (11), and from this condition we derive the value of the rate parameter α_v , which determines the internal reallocation of N to active mycelium through vacuolisation,

$$\alpha_{v} = \frac{\epsilon \rho_{1}(D_{1} + D_{2} + D_{3}) + \phi_{min} - D_{1} \frac{L_{hN}}{L_{hC}} - D_{3} \frac{F_{nN}}{F_{nC}}}{F_{cC} \left(\rho_{1} - \rho_{2}\right)}.$$
 (12)

Here ϕ_{min} is negative (or zero) and represents the capacity of the external environment to provide N for mycelial uptake (i.e. N import). In summary, low litter N content (unless compensated by N import) leads to positive values of α_v (fungal vacuolisation) and negative values of ϕ . As decomposition progresses and the litter (including fungal necromass) is progressively enriched in N to fulfill the fungal requirements, the system reaches a critical point at which α_v is zero and ϕ becomes positive. This balance point is when the fungus reaches its stoichiometric balance (C and N co-limitation).

2.3. Model parametrisation and goodness of fit

The model was tested using two different datasets from Berg and McClaugherty (1989) and Osono and Takeda (2004) to evaluate the model sensitivity to litter N content within a single plant species and across species. We choose to use data from common garden experiments to eliminate site-dependent factors, such as soil temperature and moisture, which are not represented in our model.

The dataset from Berg and McClaugherty (1989) includes changes in mass loss and N content of litter from a single species (*Pinus silvestris L.*). Two types of litter were selected, either from fertilised trees (initial N:C=0.016) or from non-fertilised trees (initial N:C=0.008), with similar initial lignin content (267, 268 mg/g). The litter was collected and incubated in a boreal Scots pine forest near Jädraås, Sweden. Litters were incubated in mesh bags and retrieved multiple times during a 48 weeks incubation period.

The second dataset from Osono and Takeda (2004) includes mass loss and N content data of plant litters across different species with different initial N content, but similar lignin content (Osono and Takeda, 2004); the original data was kindly provided by T. Osono. The experiment was conducted in the cool temperate deciduous Ashiu Experimental Forest, Japan on two nearby sites along a hillslope. The data used for model calibration was from the upper site (decomposition at the lower site was very similar) and we selected five litter species: *Pterostyrax*

Table 2

Fluxes (mg d^{-1})	Description	Mathematical formulation
D_1	Decomposition rate of hydrolysable C	$D_{max_1} \frac{L_{hC} F_{eC}}{K(L_{hC} + L_{\rho C} + F_{nC}) + F_{eC} + F_{\nu C}}$
D_2	Decomposition rate of oxidisable C	$D_{max_2} \frac{L_{oC} F_{cC}}{K(L_{hC} + L_{oC} + F_{nC}) + F_{cC} + F_{vC}}$
D_3	Decomposition rate of fungal necromass	$D_{max_3} \frac{F_{nC} F_{cC}}{K(L_{hC} + L_{oC} + F_{nC}) + F_{cC} + F_{vC}}$
M_c	Proportional mortality rate of cytoplasmic mycelium	$\alpha_m F_{cC}$,
M_v	Proportional mortality rate of vacuolised mycelium	$\alpha_m F_{vC}$,
M_s	Senescence mortality rate of vacuolised mycelium	$\beta V, \forall \beta \in [0,1]$
V	Vacuolisation rate	$lpha_v F_{cC}$
ϕ	Net N mineralisation rate	Equation (11)

Table 3

Parameters	Description	Units
D_{max_1}	Decomposition rate constant of hydrolysable C	
D_{max_2}	Decomposition rate constant of non-hydrolysable C	d^{-1}
D_{max_3}	Decomposition rate constant of fungal Necromass	d^{-1}
K	Half saturation constant	_
α_m	Proportional mortality rate constant	d^{-1}
ϵ	Carbon use efficiency	_
β	Senescence mortality rate constant	d^{-1}
α_v	Vacuolisation rate (dynamic under N limitation (12))	d^{-1}
ρ_1	N:C ratio of cytoplasmic mycelium	
ρ_2	N:C ratio of vacuolised mycelium	mgN mgC ⁻¹
ϕ_{min}	Capacity of environment to deliver N for immobilisation	$mgN d^{-1}$

hispida (initial N:C=0.053), Castanea crenata (initial N:C=0.019), Magnolia obovata (initial N:C=0.016), Acer mono var (initial N:C=0.015), Cryptomeria japonica (initial N:C=0.009), out of 14 litters with an initial lignin content within the narrow range of 300–400 mg/g, since our model does not feature lignin-N interactions. The litters were incubated in mesh bags, which were retrieved at different times during a 35 month incubation period.

The mycelial N:C ratios $\rho_1=0.100$ and $\rho_2=0.033$ were estimated based on Fig3.b in Högberg et al. (2021), who observed C:N ratios of mycelium (of ectomycorrhizal fungi) ranging between 10 and 30 over a gradient in N availability.

CUE (ϵ) was estimated separately for each dataset. The total amount of N in the litter bags peaks when the litter N:C is equal to the threshold element ratio at which net N mineralisation is zero. Therefore, at the peak, litter N:C = $\rho_1\epsilon$, so that CUE can be estimated as ϵ =litter N:C ρ_1^{-1} . Based on this calculation and ρ_1 , the CUE (ϵ) was estimated to 0.16 from Berg and McClaugherty (1989) and 0.39 from Osono and Takeda (2004). The estimated value from Berg and McClaugherty (1989) dataset is in line with estimates for fungus Mycena epipterygia decomposing pine litter (Boberg et al., 2014) and the latter aligns with estimates provided for more N-rich litter using both empirical and theoretical approaches (Manzoni, 2017).

 ϕ_{min} was estimated separately for each dataset based on the linear rate of N import into the most N poor litter (until peak N).

Furthermore, proportional mortality (α_m) is a highly uncertain parameter and there is little available data. Thus, for each dataset we adjusted (α_m) such that the microbial biomass was roughly 1% of the organic matter as commonly observed e.g. in Clemmensen et al. (2013); 0.1 d^{-1} for Osono and Takeda (2004) and 0.015 d^{-1} for Berg and McClaugherty (1989). Rates of mortality of 0.02 d^{-1} or lower were observed for mycorrhizal mycelium in boreal forest (Hagenbo et al., 2017) and higher rates in temperate ecosystems seem reasonable. The half saturation constant K was chosen to be approximately equal to the fungal biomass content of litter (i.e. 1%), to attain a reasonable saturation effect. We solved the model numerically using initial conditions for the litter pools estimated from each dataset separately. We used initial lignin content only to initialise the model, because the measured data from later decomposition stages also includes the recalcitrant fraction of fungal necromass, but in our model necromass is not divided into fast

and slow decomposing pools. Simulations were initialised with a small fungal biomass pool. Both datasets were normalised to 1 g of initial C. Parameters were calibrated by fitting the model to data on total C and N at different times of incubation, using the Generalised Likelihood Uncertainty Estimation (GLUE) approach (Beven and Binley, 1992, 2014; Beven, 2006), which assigns likelihoods to different parameter sets to produce best predictions. To cover the maximum range of parameters, a sampling space of 100000 samples was generated by Latin hypercube sampling using the *Ihsdesign* function in MATLAB (R2023a). A numerical solution of our model system (1)–(9) was obtained using the solver *ode45* in MATLAB for each parameter set. To identify the best parameter set, we employed the Nash–Sutcliffe Efficiency (NSE) criterion.

$$NSE = 1 - \frac{\sum_{i} (X_{i} - Y_{i})^{2}}{\sum_{i} (X_{i} - \overline{X_{i}})^{2}}$$
 (13)

where X_i represents the observed data, Y_i represents the corresponding model predicted values, $\overline{X_i}$ represents the mean of observed data and NSE $\in [0,1]$. A NSE value closer to 1 indicates a better model fit. The best simulation of our model system was selected based on the maximum NSE obtained after averaging NSE for C and N data.

3. Results

3.1. Necessary conditions for fungal growth

Our model describes mycelial dynamics that allow fungi to decompose N poor litter, but even with such adaptations there is a lower limit of litter N content below which decomposition cannot occur. This limit, in turn, depends on specific fungal traits and inorganic N availability. We derived an expression for the lowest possible initial litter N:C ratio at which decomposition can start for a given rate of vacuolisation (α_v) at t=0, by substituting decomposition rates (Eq. (10)) into Eq. (12) and solving it for litter N:C ($\frac{L_{hN}}{L_{hC}+L_{pC}}$).

$$\min \frac{L_{hN}}{L_{hC} + L_{oC}} = \frac{\epsilon \rho_1 (D_{max_1} L_{hC} + D_{max_2} L_{oC})}{D_{max_1} (L_{hC} + L_{oC})} + \left(\frac{K + \frac{F_{cC}}{L_{hC} + L_{oC}}}{D_{max_1}}\right) \left[\frac{\phi_{min}}{F_{cC}} - (\rho_1 - \rho_2)\alpha_{\nu}\right].$$
(14)

Table 4
Parameter values

Parameter	Value Berg and McClaugherty (1989)	Value Osono and Takeda (2004)	Source
α_m	$0.015 \ d^{-1}$	$0.1 \ d^{-1}$	chosen value
ρ_1	0.1 mgN mgC ⁻¹	0.1 mgN mgC^{-1}	based on Högberg et al. (2021)
ρ_2	0.033 mgN mgC ⁻¹	0.033 mgN mgC ⁻¹	based on Högberg et al. (2021)
ϵ	0.16	0.39	calculated from Berg and McClaugherty (1989) and Osono and Takeda (2004)
K	0.01	0.01	chosen value
ϕ_{min}	$-0.0009 \text{ mgN } d^{-1}$	$-0.008 \text{ mgN } d^{-1}$	calculated from Berg and McClaugherty (1989) and Osono and Takeda (2004)
D_{max_1}	$0.0043 \ d^{-1}$	$0.011 \ d^{-1}$	calibrated
D_{max_2}	$0.00044 \ d^{-1}$	$0.0033 \ d^{-1}$	calibrated
D_{max_3}	$0.0011 \ d^{-1}$	$0.0041 \ d^{-1}$	calibrated
β	$0.31 \ d^{-1}$	$0.25 \ d^{-1}$	calibrated

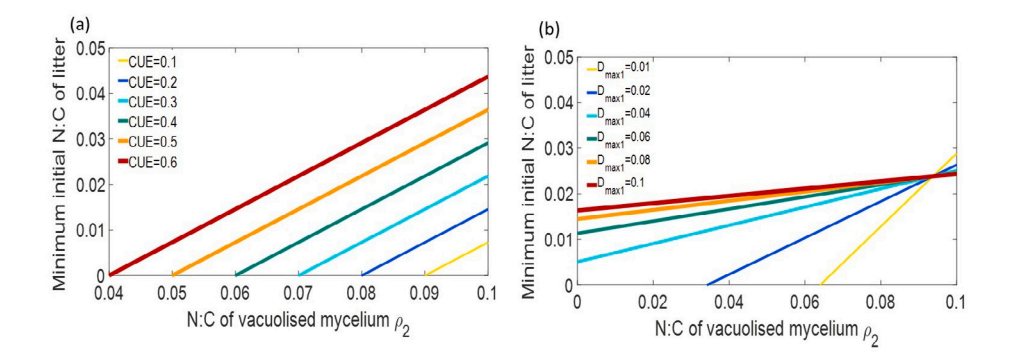


Fig. 3. A low initial N content of the litter can be tolerated by reducing CUE (a), by reducing the decomposition rate of the hydrolysable pool D_{max_1} (b), or by lowering the N:C of the vacuolised mycelium (a), (b). The vacuolisation rate α_n is set to 0.8.

This equation shows that decomposition of litter with low initial N:C ratio is possible only with low CUE (ϵ ; Fig. 3a), low ϕ_{min} , and/or ρ_2 . Note that ϕ_{min} is negative, and lower values (more negative) indicate more higher N import from external sources. Fungi can adapt to a low initial litter N content by reducing ρ_2 (Fig. 3a-b), by slowing down decomposition (Fig. 3b), by speeding up vacuolisation, or by importing more N if it is available.

3.2. Model predictions

In our model describing three different fractions of fungal mycelium (active, vacuolised, and dead), fungi adapt to N scarcity by increasing the proportion of vacuolised cells, which are inactive and N poor, consequently reducing decomposition rates. While the mechanism of response to N limitation is described in the model, the rate constants in the decomposition kinetics still need to be calibrated. These rate constants and senescence mortality were estimated using the GLUE method and data on litter C and N dynamics from Berg and McClaugherty (1989) (litters from a single plant species from different fertilisation treatments) and Osono and Takeda (2004) (multiple species). After calibration, Nash-Sutcliffe model efficiencies were as high as 0.94 and 0.87, respectively. Thus, our model can effectively predict mass loss of litters of different quality within a species as well as cross-species litter variation. The parameter sets obtained from two calibrations are given in Table 4. The estimated maximum decomposition rates $(D_{max_1}, D_{max_2}, D_{max_3})$ differ between datasets, with lower values under boreal conditions in Berg and McClaugherty (1989) compared with the temperate conditions of Osono and Takeda (2004). The senescence mortality rate β was quite similar between the two datasets.

The results of a single parameter set (Table 4) for each dataset are presented in Fig. 4, where the colour gradient indicates different litter types based on their initial N content, from N-rich (red) to N-poor (blue). The temporal decline in litter total C is illustrated in Fig. 4a, 4f, indicated by mass loss trajectories predicted based on model simulations with observed data included for comparison. The model predicts

slower decomposition of N-poor litters. Litter N increases linearly for litters with lower initial N content at the initial stage of decomposition due to N import, i.e as $\phi = \phi_{min}$ (which is negative indicating N import) and attains maxima at later time points. Only for the N-rich litters (in red), a lack of vacuolisation leads to fast decomposition and N release already from the start (positive ϕ). After switching from N-limitation (N import) to C-limitation (N losses), all trajectories exhibit a convergence towards a similar N pool (Fig. 4b, 4g).

Lower N availability leads to a higher proportion of inactive, vacuolised mycelium linked to a lower total mycelial N content (Fig. 4c, d, h, i). Fig. 4e, 4j illustrates the temporal dynamics of fungal biomass. C acquisition and fungal biomass accumulation are delayed by a lower N content of mycelium due to a higher proportion of inactive cells. Biomass dynamics also depends on proportional mortality α_m , which was chosen such that the fungal biomass varies around 10 mg fungal C per gram litter C. The calibrated necromass decomposition rate (D_{max_3}) for both datasets is slower than the decomposition rate of the hydrolysable pool (cellulose and proteins) and more similar to the decomposition rate of the oxidisable pool (Table 4).

3.3. Sensitivity analysis

We carried out a sensitivity analysis on most of the parameters in the model by changing the original values by $\pm 40\%$ to determine the effect of parameter modulation on the temporal dynamics of litter C, N pools and the proportion of inactive mycelium (Fig. 5, supplementary Fig. S1). For β , we instead tested values of 0 and 1. The sensitivity analysis was performed for two litter types, the most N-rich litter (green lines in Fig. 5) and the most N-poor litter (blue lines) from Osono and Takeda (2004). One parameter at a time was varied while keeping the other parameters fixed.

C dynamics of the N-poor litter is highly sensitive to CUE (ϵ). High CUE induces stronger N limitation, which in turns reduces fungal biomass accumulation, and leads to a higher fraction of inactive mycelium (Fig. 5c) and slower C loss (Fig. 5a). In contrast, the effect

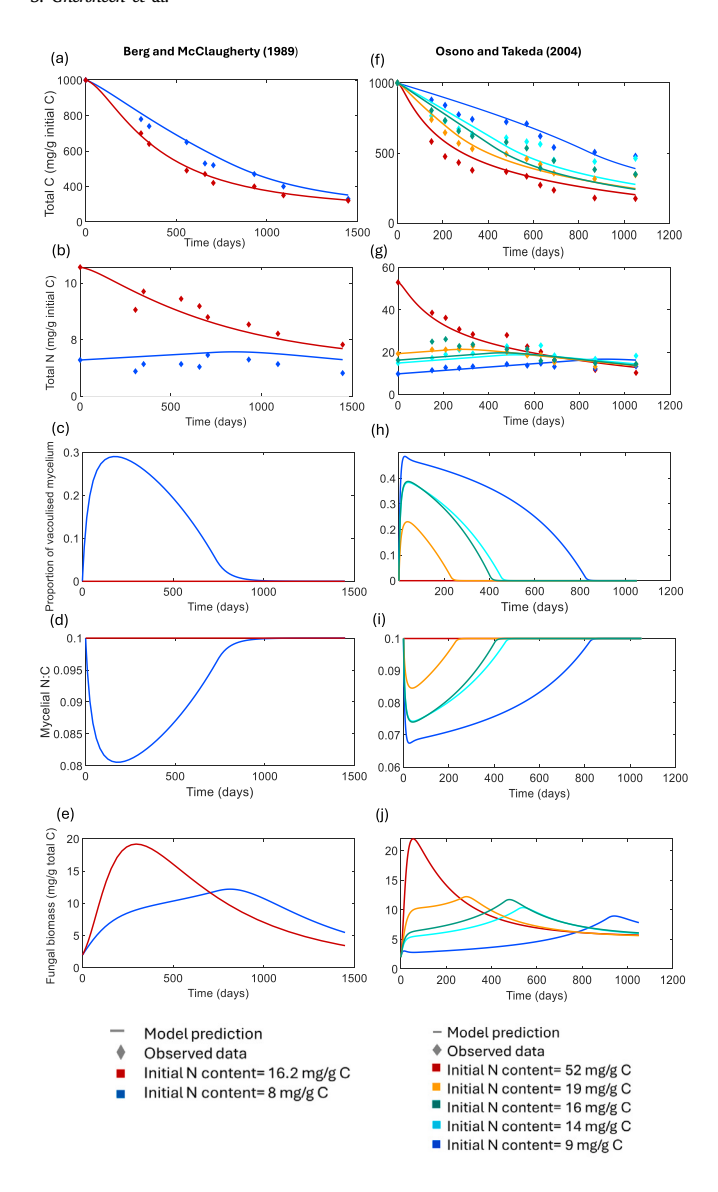


Fig. 4. Model predictions using a single parameter set for each dataset with different initial N content. N-poor litters exhibit slower mass loss (a, f), a longer period of N import, and delayed N mineralisation (b, g). Lower N availability leads to a higher proportion of inactive mycelium (c, h), which lowers the total N content of the mycelium (d, i), resulting in delayed and lower proliferation of fungal biomass (e, i)

of CUE on C dynamics was small in N-rich litter (Fig. 5a), whereas N release from N-rich litter was slower at high CUE.

As expected, the C and N dynamics are affected by the decomposition rate constant of the hydrolysable pool (D_{max_1}), but the trends caused by varying this parameter remained consistent between N rich and N poor litters (Fig. 5d, e, f). The parameter D_{max_1} does not affect the N dynamics of N-poor litter, which depends only on N import (ϕ_{min}). In N poor litter, higher D_{max_1} increases the proportion of inactive mycelium at early stages of decomposition (Fig. 5f).

The decomposition rate of necromass (D_{max_3}) had a larger impact on model predictions at late decomposition stages (Fig. 5g, h, i). For low D_{max_3} , indicating lower fungal N recycling from necromass, larger amounts of fungal necromass accumulate at the late stage of decomposition. Modulating senescence mortality had marginal effect on model predictions (Fig. 5j, 5k).

4. Discussion

4.1. Mycelial dynamics explain nitrogen limitation

We designed a litter decomposition model to investigate effects of N limitation with the focus on fungal mycelial dynamics, while keeping CUE fixed and enzyme production implicit in the decomposition kinetics. We found that mycelial dynamics - specifically N reallocation within the mycelium through the formation of N-poor, vacuolised cells - was sufficient for explaining variation in mass loss as well as N accumulation and release during decomposition of a variety of plant litters with contrasting N content, either due to fertilisation or intraspecific variation. Our model provides quantitative evidence that formation of inactive, vacuolised cells allows fungi to cope with low N availability during the initial stages of plant litter decomposition. The formation of vacuolised mycelium might, thus, be an important adjustment of fungi to live in N-poor ecosystems, such as boreal forests. An advantage of our model lies in its ability to accurately predict litter decomposition patterns using a small set of general parameters, instead of estimating different parameter sets for different litters. Furthermore, the fitted parameters were not directly related to the mechanisms of N limitation. but, rather, general descriptors of decomposition rates. The effect of N constraints on decomposition depended primarily on parameter values obtained from the literature (e.g. ρ_1 and ρ_2) or estimated for each location of incubation (ϵ , α_m and ϕ_{min}).

In Manzoni et al. (2021), calibrating parameters at the site level allowed capturing of overall decomposition patterns across litter types, but often N accumulation was underestimated and N mineralisation overestimated regardless of which microbial strategy to deal with N limitation was tested. This might be due to the wider range of litter types considered in that study, which inevitably introduces sources of variability compared to the smaller dataset used here (e.g., a wider range of lignin contents). Alternatively, it is possible that the N limitation coping strategies implemented in the models by Manzoni et al. (2021) did not capture well the mechanisms related to mycelial morphology, which are the focus of the model presented here. In our model, two of the strategies considered in that work emerge from mycelial dynamics, instead of being imposed a priori. The microbial C:N is dynamic at the whole mycelium level according to the varying proportions of cytoplasmic and vacuolised cells (corresponding to the "plastic microbial C:N" strategy in Manzoni et al. (2021)). The fraction of fungal N that is retained in the active cells is also dynamic (corresponding to the "nutrient retention" strategy in Manzoni et al. (2021)). We would argue that letting these strategies emerge in our model provides a more realistic description of fungal responses to N limitation compared to models where individual strategies are switched on or off.

4.2. Fungal responses to nitrogen limitation

The degree of N limitation depends on the proportions of plant litter and fungal necromass utilised for fungal growth. A high proportion of N poor plant litter increases N limitation, whereas a high relative use of N rich necromass decreases N limitation and eventually leads to C limitation. In our model, N limitation manifests as hyphal vacuolisation and inactivation. Therefore, the vacuolisation rate (α_n) depends on the relative decomposition of plant cellulose (primarily a source of C) and fungal necromass (primarily a source of N). Increasing D_{max_1} and decreasing D_{max_3} increases the proportion of inactive mycelium during early stages of decomposition (Fig. 5f), because more rapid exploitation of N poor plant litter and thus higher N demand triggers vacuolisation. In most decomposition models, adaption to a low initial N content of plant litter depends on altered microbial CUE (Schimel and Weintraub, 2003) and biomass N:C ratios (Sistla et al., 2012; Fatichi et al., 2019). In our model, the capacity to decompose N poor litter (14) also depends on $\rho_1 - \rho_2$, which represents how much N is retained in the active cells compared to the vacuolised ones (and also on ϕ_{min} , representing

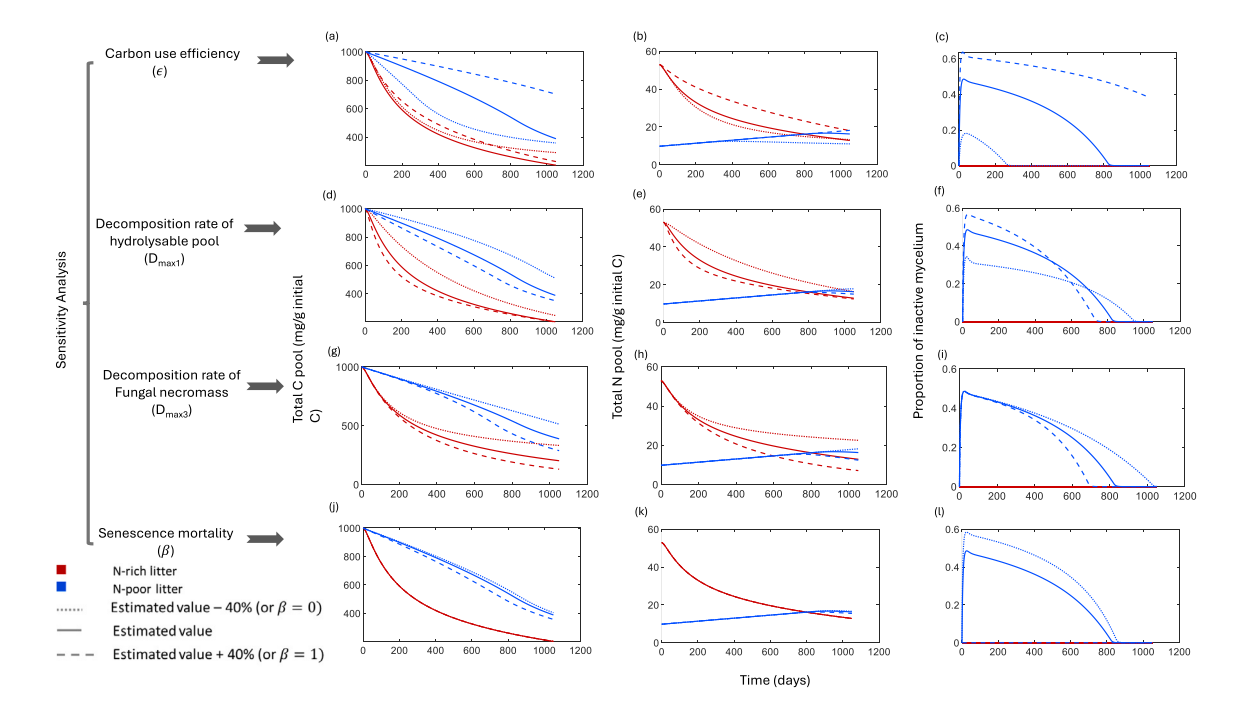


Fig. 5. Sensitivity of model predictions to carbon use efficiency (ε) (a)–(c), decomposition rate of the hydrolysable litter pool (D_{max_1}) (d)–(f), decomposition rate of the fungal necromass pool (D_{max_2}) (g)–(i) and senescence mortality (β) (j)–(l).

the availability of external N). The effect of low ρ_2 (relative to ρ_1) is stronger when growth is slow, which is evident from (14), where the second term $\left(\frac{\phi_{min}}{F_{CC}} - (\rho_1 - \rho_2)\alpha_v\right)$ decreases by the factor $\frac{1}{D_{max_1}}$ indicating that slow degradation of the hydrolysable litter pool enables more efficient N recycling. This implies that one strategy of coping with N limitation is to reduce D_{max_1} in combination with reducing ρ_2 (Fig. 3b). According to this mechanism, fungi that have to tolerate low N availability may benefit from slow growth, reflecting typical oligotrophic strategies of microorganisms (slow growth on scarce resources; (Fierer et al., 2007)). Slow growth and fast vacuolisation of mycelium enables exploration of low N resources, whereas fast growth and slow vacuolisation intensifies N-limitation, reflecting a trade-off between stress tolerance vs. resource acquisition (Malik et al., 2020).

The positive effect of CUE on N accumulation (Fig. 5b) is not surprising. Higher CUE implies faster growth, which forces microorganisms to acquire more N, leading to N limitation (Manzoni et al., 2017), which in our model triggers vacuolisation. Most important, vacuolisation is an effective way to cope with stoichiometric imbalances even if CUE is fixed (Fig. 5a). Previous work has shown that N release patterns could be explained by decreasing CUE (Manzoni et al., 2017), or increasing threshold element ratios with increasing litter C:N, which is equivalent to the CUE trend if microbial C:N is fixed (Agren et al., 2013). However, these previous works neglected reallocation and retention of N within the mycelium, which offers an alternative and under-studied avenue for coping with N limitation. Empirical studies have indicated that processes that retain nutrients in the soil microbial biomass allow bacteria and fungi to cope with unfavourable organic matter stoichiometry during decomposition (Spohn and Widdig, 2017; Boberg et al., 2014). Nutrient retention was first explored in a mathematical model by Manzoni et al. (2021), but it was parametrised through a single recycling parameter instead of adopting a process-based approach as done here. Here we go one step further by modelling the reallocation of N within the fungal mycelium as a fungal adjustment to live on N-poor substrate.

4.3. Role of fungal necromass in carbon and nitrogen cycling

In most decomposition models (with some exceptions, e.g., Sulman et al. (2017)), microbial biomass formed during decomposition is being added to the organic matter compartment when it dies. However, decomposition rates at late stages have been proposed to depend largely on microbial necromass dynamics (Sun et al., 2024), and necromass has its own distinct characteristics. Therefore, in our model, we consider plant litter and fungal necromass as separate pools. How fast fungal necromass decomposes in comparison to plant litter is still an open question (Adamczyk et al., 2019; Fernandez and Kennedy, 2018). The low estimated necromass decomposition rate (D_{max_3}) in our model indicates that fungal necromass decomposes slowly relative to hydrolysable plant litter components. One possible explanation lies in the chemical composition of fungal necromass, which often contains recalcitrant compounds, such as melanin, or may be complexed with tannins, which have a tendency to bind to proteins and chitin. These necromasstannins complexes are not easily hydrolysable and require oxidative enzymes for their degradation (Adamczyk et al., 2019). This can lead to retention of N in necromass, partially in the oxidisable pool (Baskaran et al., 2019), and the persistence of necromass in soil will delay N release. This pattern emerges in our sensitivity analysis, where higher accumulation of necromass slows down the N release from N rich litter (Fig. 5h). Furthermore, due to slow turnover of the necromass pool, there is no significant effect of senescence mortality on C and N dynamics (Fig. 5j, Fig. 5k). The predicted slow decomposition of fungal necromass is consistent with the observation that a large fraction of C in boreal forest soils is derived from fungal necromass (Clemmensen et al., 2013) and that N retention patterns depend on the dynamics of this pool (Kyaschenko et al., 2019).

4.4. Model limitations

Our model can capture decomposition patterns despite its minimal degrees of freedom, but it has some limitations. Firstly, it does not include lignin-N interactions explicitly. For this reason, we only included data from litters with a similar lignin content (but different N

contents) for model parametrisation. Yet, the content of recalcitrant compounds in litter, like lignin, is variable and has a major influence on decomposition rates (Melillo et al., 1982) and microbial biochemical activity (Chakrawal et al., 2024). Furthermore, interactions between N-limitation and different chemical litter pools are complex, with high N availability stimulating decomposition of easily degraded pools, but often retarding decomposition of recalcitrant necromass pools (Craine et al., 2007; Sun et al., 2024). The latter phenomenon is not captured by our model, so merging the interactive effects of N and non-hydrolysable compounds, particularly in necromass, would be a natural development of our model.

Secondly, we consider N import in the model by assigning a fixed value to the parameter ϕ_{min} , since the model only considers a single litter cohort with $\phi_{\it min}$ representing the N supply from the surrounding organic matrix (Boberg et al., 2014; Frey et al., 2000; Spohn and Berg, 2023). To explore patterns of resource reallocation between different substrates undergoing decomposition at the ecosystem level (Boddy, 1999), the model needs to be further developed to accommodate continuous litter inputs. This will enable modelling of resource reallocation between lower, older soil layers and fresh litter explicitly rather than via a constant rate of N import, as the capacity of more degraded material to deliver N will be incorporated in the model system. It is important to point out that some estimated parameters are site dependent, as the model does not include environmental drivers, such as temperature and moisture. CUE, mortality and external N availability are also likely to be site dependent, so the model is not directly transferable across sites without recalibration, and the purpose of this work is to illustrate a principle rather than providing predictions across sites.

5. Conclusions

We hypothesised that resource reallocation within fungal mycelium can explain the effects of low N availability on decomposition. A mathematical model developed to test this hypothesis captured decomposition patterns across litter types with different initial N content without invoking variation in CUE (between litters within sites) or selective acquisition of N, but rather predicting that N is reallocated to the growing parts of the mycelium under N limitation. This N reallocation lowers the overall fungal biomass N:C ratio, thus also reducing the fungal N demand on the expense of reduced decomposition – a mechanism not included in other biogeochemical models. Considering the benefit of explicit representation of fungal processes, we propose this framework could be effective in improving predictions of C and N cycling in N limited systems.

Mathematical analyses of the model and numerical simulations also provided insights on how fungal traits affect decomposition:

- High CUE promotes fungal growth only under high N availability, whereas in N poor conditions the higher N demand associated with high CUE triggers faster vacuolisation of mycelium, thereby slowing down decomposition.
- A trade-off emerges between fungi adapted to low N resources (slow resource acquisition and growth, but fast vacuolisation of mycelium), and fungi adapted to high N resources (fast resource acquisition and growth, but slow vacuolisation).
- Fungal necromass is chemically recalcitrant and can store large amounts of both C and N; the accumulation of N in dead mycelium can delay N release in N poor litter and slow down the N release from N rich litter.

CRediT authorship contribution statement

Samia Ghersheen: Writing – review & editing, Writing – original draft, Visualization, Validation, Software, Methodology, Investigation,

Formal analysis, Conceptualization. **Stefano Manzoni:** Conceptualization, Writing – review & editing, Supervision, Funding acquisition. **Marie Spohn:** Writing – review & editing, Funding acquisition, Conceptualization. **Björn D. Lindahl:** Project administration, Funding acquisition, Formal analysis, Conceptualization, Writing – review & editing, Writing – original draft, Supervision.

Funding

This project has received funding from the Swedish Research Council Vetenskapsradet, Sweden (grant 2020-03910), and the Swedish Research Council FORMAS, Sweden (grant 2021-02121).

Declaration of competing interest

The authors declare that they have no known competing financial interests or personal relationships that could have appeared to influence the work reported in this paper.

Acknowledgement

We thank T. Osono for sharing litter decomposition data.

Appendix A. Supplementary data

Supplementary material related to this article can be found online at https://doi.org/10.1016/j.soilbio.2025.109899.

Data availability

The MATLAB code of GLUE method for model parametrisation is available at https://doi.org/10.5281/zenodo.15464600.

References

- Adamczyk, B., Sietiö, O.-M., Biasi, C., Heinonsalo, J., 2019. Interaction between tannins and fungal necromass stabilizes fungal residues in boreal forest soils. New Phytol. 223 (1), 16–21.
- Agren, G.I., Hyvönen, R., Berglund, S.L., Hobbie, S.E., 2013. Estimating the critical N: C from litter decomposition data and its relation to soil organic matter stoichiometry. Soil Biol. Biochem. 67, 312–318.
- Baldrian, P., 2017. Forest microbiome: diversity, complexity and dynamics. FEMS Microbiol. Rev. 41 (2), 109–130.
- Baldrian, P., Větrovský, T., Cajthaml, T., Dobiášová, P., Petránková, M., Šnajdr, J., Eichlerová, I., 2013. Estimation of fungal biomass in forest litter and soil. Fungal Ecol. 6 (1), 1–11.
- Baskaran, P., Ekblad, A., Soucemarianadin, L.N., Hyvönen, R., Schleucher, J., Lindahl, B.D., 2019. Nitrogen dynamics of decomposing Scots pine needle litter depends on colonizing fungal species. FEMS Microbiol. Ecol. 95 (6), fiz059.
- Berg, B., McClaugherty, C., 1989. Nitrogen and phosphorus release from decomposing litter in relation to the disappearance of lignin. Can. J. Bot. 67 (4), 1148–1156.
- Berg, B., McClaugherty, C., 2008. Plant Litter: Decomposition, Humus Formation, Carbon Sequestration. Springer, Berlin.
- Beven, K., 2006. A manifesto for the equifinality thesis. J. Hydrol. 320 (1–2), 18–36.
 Beven, K., Binley, A., 1992. The future of distributed models: model calibration and uncertainty prediction. Hydrol. Process. 6 (3), 279–298.
- Beven, K., Binley, A., 2014. GLUE: 20 years on. Hydrol. Process. 28 (24), 5897–5918.
 Boberg, J.B., Finlay, R.D., Stenlid, J., Ekblad, A., Lindahl, B.D., 2014. Nitrogen and carbon reallocation in fungal mycelia during decomposition of boreal forest litter.
 PLoS One 9 (3), e92897.
- Boddy, L., 1999. Saprotrophic cord-forming fungi: meeting the challenge of heterogeneous environments. Mycologia 91 (1), 13–32.
- Boswell, G.P., Jacobs, H., Davidson, F.A., Gadd, G.M., Ritz, K., 2002. Functional consequences of nutrient translocation in mycelial fungi. J. Theoret. Biol. 217 (4), 459–477.
- Bradford, M.A., Veen, G.F., Bonis, A., Bradford, E.M., Classen, A.T., Cornelissen, J.H.C., Crowther, T.W., De Long, J.R., Freschet, G.T., Kardol, P., Manrubia-Freixa, M., 2017. A test of the hierarchical model of litter decomposition. Nat. Ecol. Evol. 1 (12), 1836–1845.
- Camenzind, T., Mason-Jones, K., Mansour, I., Rillig, M.C., Lehmann, J., 2023. Formation of necromass-derived soil organic carbon determined by microbial death pathways. Nat. Geosci. 16 (2), 115–122.

- Camenzind, T., Philipp Grenz, K., Lehmann, J., Rillig, M.C., 2021. Soil fungal mycelia have unexpectedly flexible stoichiometric C: N and C: P ratios. Ecol. Lett. 24 (2), 208–218
- Chakrawal, A., Lindahl, B.D., Manzoni, S., 2024. Modelling optimal ligninolytic activity during plant litter decomposition. New Phytol. 243 (3), 866–880.
- Clemmensen, K.E., Bahr, A., Ovaskainen, O., Dahlberg, A., Ekblad, A., Wallander, H., Stenlid, J., Finlay, R.D., Wardle, D.A., Lindahl, B.D., 2013. Roots and associated fungi drive long-term carbon sequestration in boreal forest. Science 339 (6127), 1615–1618.
- Craine, J.M., Morrow, C., Fierer, N., 2007. Microbial nitrogen limitation increases decomposition. Ecology 88 (8), 2105–2113.
- Dowson, C.G., Springham, P., Rayner, A.D.M., Boddy, L., 1989. Resource relationships of foraging mycelial systems of Phanerochaete velutina and Hypholoma fasciculare in soil. New Phytol. 111 (3), 501–509.
- Falconer, R.E., Bown, J.L., White, N.A., Crawford, J.W., 2005. Biomass recycling and the origin of phenotype in fungal mycelia. Proc. R. Soc. B: Biol. Sci. 272 (1573), 1727–1734.
- Falconer, R.E., Bown, J.L., White, N.A., Crawford, J.W., 2007. Biomass recycling: a key to efficient foraging by fungal colonies. Oikos 116 (9), 1558–1568.
- Fatichi, S., Manzoni, S., Or, D., Paschalis, A., 2019. A mechanistic model of microbially mediated soil biogeochemical processes: a reality check. Glob. Biogeochem. Cycles 33 (6), 620–648.
- Fernandez, C.W., Kennedy, P.G., 2018. Melanization of mycorrhizal fungal necromass structures microbial decomposer communities. J. Ecol. 106 (2), 468–479.
- Fierer, N., Bradford, M.A., Jackson, R.B., 2007. Toward an ecological classification of soil bacteria. Ecology 88 (6), 1354–1364.
- Frey, S.D., Elliott, E.T., Paustian, K., Peterson, G.A., 2000. Fungal translocation as a mechanism for soil nitrogen inputs to surface residue decomposition in a no-tillage agroecosystem. Soil Biol. Biochem. 32 (5), 689–698.
- Fricker, M.D., Heaton, L.L., Jones, N.S., Boddy, L., 2017. The mycelium as a network. Fungal Kingd. 335–367.
- Guhr, A., Borken, W., Spohn, M., Matzner, E., 2015. Redistribution of soil water by a saprotrophic fungus enhances carbon mineralization. Proc. Natl. Acad. Sci. 112 (47), 14647–14651.
- Hagenbo, A., Clemmensen, K.E., Finlay, R.D., Kyaschenko, J., Lindahl, B.D., Fransson, P., Ekblad, A., 2017. Changes in turnover rather than production regulate biomass of ectomycorrhizal fungal mycelium across a Pinus sylvestris chronosequence. New Phytol. 214 (1), 424–431.
- Högberg, M.N., Högberg, P., Wallander, H., Nilsson, L.O., 2021. Carbon-nitrogen relations of ectomycorrhizal mycelium across a natural nitrogen supply gradient in boreal forest. New Phytol. 232 (4), 1839–1848.
- Kyaschenko, J., Ovaskainen, O., Ekblad, A., Hagenbo, A., Karltun, E., Clemmensen, K.E., Lindahl, B.D., 2019. Soil fertility in boreal forest relates to root-driven nitrogen retention and carbon sequestration in the mor layer. New Phytol. 221 (3), 1492–1502
- Lindahl, B.D., Olsson, S., 2004. Fungal translocation-creating and responding to environmental heterogeneity. Mycologist 18 (2), 79–88.
- Lindahl, B.O., Taylor, A.F., Finlay, R.D., 2002. Defining nutritional constraints on carbon cycling in boreal forests-towards a lessphytocentric'perspective. Plant Soil 242 (1), 123–135.
- Malik, A.A., Martiny, J.B., Brodie, E.L., Martiny, A.C., Treseder, K.K., Allison, S.D., 2020. Defining trait-based microbial strategies with consequences for soil carbon cycling under climate change. ISME J. 14 (1), 1–9.
- Manzoni, S., 2017. Flexible carbon-use efficiency across litter types and during decomposition partly compensates nutrient imbalances—results from analytical stoichiometric models. Front. Microbiol. 8, 661.
- Manzoni, S., Čapek, P., Mooshammer, M., Lindahl, B.D., Richter, A., Šantrůčková, H., 2017. Optimal metabolic regulation along resource stoichiometry gradients. Ecol. Lett. 20 (9), 1182–1191.

- Manzoni, S., Chakrawal, A., Spohn, S.M., Lindahl, B.D., 2021. Modeling microbial adaptations to nutrient limitation during litter decomposition. Front. For. Glob. Chang. (4), 686945.
- Manzoni, S., Trofymow, J.A., Jackson, R.B., Porporato, A., 2010. Stoichiometric controls on carbon, nitrogen, and phosphorus dynamics in decomposing litter. Ecol. Monograph. 80 (1), 89–106.
- Melillo, J.M., Aber, J.D., Muratore, J.F., 1982. Nitrogen and lignin control of hardwood leaf litter decomposition dynamics. Ecology 63 (3), 621–626.
- Moorhead, D.L., Lashermes, G., Sinsabaugh, R.L., Weintraub, M.N., 2013. Calculating co-metabolic costs of lignin decay and their impacts on carbon use efficiency. Soil Biol. Biochem. 66, 17–19.
- Mooshammer, M., Wanek, W., Zechmeister-Boltenstern, S., Richter, A., 2014. Stoichiometric imbalances between terrestrial decomposer communities and their resources: mechanisms and implications of microbial adaptations to their resources. Front. Microbiol. 5, 22.
- Osono, T., Takeda, H., 2004. Accumulation and release of nitrogen and phosphorus in relation to lignin decomposition in leaf litter of 14 tree species. Ecol. Res. 19, 593-602
- Parton, W.J., Scurlock, J.M.O., Ojima, D.S., Gilmanov, T.G., Scholes, R.J., Schimel, D.S., Kirchner, T., Menaut, J.C., Seastedt, T., García Moya, E., Kamnalrut, A., 1993. Observations and modeling of biomass and soil organic matter dynamics for the grassland biome worldwide. Glob. Biogeochem. Cycles 7 (4), 785–809.
- Schimel, J.P., Weintraub, M.N., 2003. The implications of exoenzyme activity on microbial carbon and nitrogen limitation in soil: a theoretical model. Soil Biol. Biochem. 35 (4), 549–563.
- Sistla, S.A., Asao, S., Schimel, J.P., 2012. Detecting microbial N-limitation in tussock tundra soil: implications for Arctic soil organic carbon cycling. Soil Biol. Biochem. 55, 78–84.
- Sistla, S.A., Rastetter, E.B., Schimel, J.P., 2014b. Responses of a tundra system to warming using SCAMPS: a stoichiometrically coupled, acclimating microbe-plant-soil model. Ecol. Monograph. 84 (1), 151–170.
- Spohn, M., Berg, B., 2023. Import and release of nutrients during the first five years of plant litter decomposition. Soil Biol. Biochem. 176, 108878.
- Spohn, M., Widdig, M., 2017. Turnover of carbon and phosphorus in the microbial biomass depending on phosphorus availability. Soil Biol. Biochem. 113, 53–59.
- Sulman, B.N., Brzostek, E.R., Medici, C., Shevliakova, E., Menge, D.N., Phillips, R.P., 2017. Feedbacks between plant N demand and rhizosphere priming depend on type of mycorrhizal association. Ecol. Lett. 20 (8), 1043–1053.
- Sun, T., Dong, L., Zhang, Y., Hättenschwiler, S., Schlesinger, W.H., Zhu, J., Berg, B., Adair, C., Fang, Y., Hobbie, S.E., 2024. General reversal of N-decomposition relationship during long-term decomposition in boreal and temperate forests. Proc. Natl. Acad. Sci. 121 (20), e2401398121.
- Tang, J.Y., Riley, W.J., 2013. A total quasi-steady-state formulation of substrate uptake kinetics in complex networks and an example application to microbial litter decomposition. Biogeosciences 10 (12), 8329–8351.
- Tipping, E., Somerville, C.J., Luster, J., 2016. The C: N: P: S stoichiometry of soil organic matter. Biogeochemistry 130, 117–131.
- Tlalka, M., Bebber, D.P., Darrah, P.R., Watkinson, S.C., Fricker, M.D., 2008. Quantifying dynamic resource allocation illuminates foraging strategy in Phanerochaete velutina. Fungal Genet. Biol. 45 (7), 1111–1121.
- Veses, V., Richards, A., Gow, N.A., 2008. Vacuoles and fungal biology. Curr. Opin. Microbiol. 11 (6), 503-510.
- Wardle, D.A., Hornberg, G., Zackrisson, O., Kalela-Brundin, M., Coomes, D.A., 2003. Long-term effects of wildfire on ecosystem properties across an island area gradient. Science 300 (5621), 972–975.